Hindawi
Geofluids
Volume 2023, Article ID 1661379, 24 pages
https://doi.org/10.1155/2023/1661379

Research Article

Prediction Method of Vertical Ultimate Compressive Bearing Capacity of Single Pile in Soft Soil considering the Influence of Gravity

Kevin Xiao, Shihong Guo, Jianghai Wen, Jingbo Han, and Xiong Yang

School of Civil Engineering, Xi'an University of Architecture and Technology, Xi'an 710055, China

Correspondence should be addressed to Kevin Xiao; kevinx@xauat.edu.cn

Received 9 September 2022; Revised 1 October 2022; Accepted 10 October 2022; Published 25 April 2023

Academic Editor: Dongjiang Pan

Considering that the pile foundation is widely used in soft soil, in order to improve the prediction accuracy of the vertical ultimate compressive bearing capacity of a single pile, this paper puts forward a calculation model of the pile side friction resistance in homogeneous soil based on the previous research and further deduces the calculation method of pile body internal force in layered soil under the influence of gravity field. In this research, the transmission of load along the pile body is related to the previous research on the ultimate end resistance, and an analytical calculation for the vertical ultimate compressive capacity of a single pile is proposed. The novelty of the method is that the ultimate bearing capacity is solved from the perspective of force transfer while considering its own gravity, making the results more accurate. In order to verify the reliability of the method, four engineering test piles in the soft soil area of Suzhou, China, were selected, and it is indicated that the results of the static load test and finite element simulation are consistent with the proposed method, proving that the method proposed in this paper for predicting the vertical ultimate compressive bearing capacity of single pile in soft soil area has an excellent effect.

1. Introduction

As a bearing structure, the pile is widely used in foundation reinforcement, and predicting pile bearing capacity is essential to work. Predecessors have done much research on this [1–4]. Conte et al. [5] proposed a simple method to evaluate the bearing capacity of piles under oblique loads. Liu et al. [6] deduced the calculation method of bearing capacity of Single Squeezed Branch Pile based on the load transfer method. Guo et al. proposed a method for calculating the ultimate vertical bearing capacity of SDRN piles considering two damage modes [7]. Pu et al. proposed a method for calculating the ultimate bearing capacity of uplifted piles in geotechnical bodies [8]. The above methods promote the progress of the prediction level of ultimate bearing capacity of monopiles, but do not sufficiently consider the influence of the pile's gravity. In addition, some researchers have also used artificial intelligence techniques to establish the ultimate bearing capacity prediction models [9–14], and these methods do not require specific formulas and thus have convenient features. However, the establishment and development of prediction models require the collection of a sufficient number of valid test data.

Numerical simulations are also an important way to study the load-carrying capacity of piles [15–17]. Kong et al. used FLAC 3D numerical modeling technique to gain insight into the load carrying capacity of wedge piles [18], and the results showed that the expanded bottom wedge pile is a cost-effective pile that can improve the vertical load carrying capacity under compressive and pullout loads. Elsherbiny and Naggar evaluated the compressive capacity and load transfer mechanism of helical piles in sand and clay using a validated finite element model [19]. Saggu and Chakraborty investigated the interaction between energy piles and soil in sandy soils using the finite element software Abaqus to explore the factors influencing the bearing capacity [20]. Nowkandeh and

Choobbasti used finite element (FE) models to study the axial compressive performance of helical piles in sandy and cohesive soils, obtained the failure mechanism of pile groups, and provided recommendations for the design of helical pile groups using analytical equations [21]. Although the numerical simulation approach can provide more comprehensive data on the piles when they are subjected to loads, the modeling is generally complex and requires a reasonable intrinsic model to be assigned to each entity [22–25].

A static load test is common and effective for predicting bearing capacity at construction sites [26, 27]. Mishra [28] summarized and compared the results of load settlement curves in static load tests in the Bombay area with methods for predicting the ultimate bearing capacity of rock-inlaid piles such as De Beer's method (1967) [29], Chin-Kondner Extrapolation method (1970) [30], Decourt's method (1999) [31]. Alielahi and Adampira [32] compared the results of static load test load settlement curves based on the Shahid Rajaee Port Complex Development Project in the south of Iran case study between the API [33] method and AASHTO [34] method for predicting the bearing capacity of monopiles. In general, the static load test is a costly and has a delayed prediction method. The prediction of the ultimate bearing capacity of monopiles based on the load tests of CPT and CPTU is a simple and fast prediction method [35–38]. Two parameters, cone tip resistance and sidewall resistance, are obtained from the CPT tests, which can be used to classify the soil layers and estimate the strength and deformation characteristics of the soil at different depths to provide data support for the ultimate load capacity prediction. However, the final ultimate bearing capacity prediction results are derived from empirically generated equations, and empirical values are often a major source of error.

Soft soil is an inevitable form of soil. The poor bearing capacity of foundation in soft soil areas is an important reason for some engineering accidents. Whether some of the above methods can meet the accuracy requirements for predicting the monopile bearing capacity in soft soil areas needs to be further verified. The purpose of this paper is to propose a method for predicting the ultimate bearing capacity of monopiles suitable for the prediction accuracy in soft soil areas from the perspective of force transfer and considering the influence of the pile's own gravity.

The research line of this paper starts from the characteristics of load transfer mode and pile end damage. The method of Randolph [39] can well express the transfer law of pile top load along the pile body. Based on this, the author considered the limit pile lateral friction resistance limit, considered the effect of gravity, and proposed a pile lateral friction resistance calculation model for pile sections in homogeneous soil. In this paper, this calculation model is introduced into the laminated soil, thus further revealing the transfer law of pile top load along the pile body in the laminated soil. When piles in soft soil areas are subjected to ultimate loads, the soil at the pile end undergoes a severe squeezing tendency, and Janbu [40] proposed pile end deformation characteristics that match this. Its ultimate end resistance calculation method can be well coupled with the force characteristics of the pile in the upper soft soil region when the overall shear deformation occurs. The author establishes a unified connection between the above-mentioned transfer law of pile top load and the study of ultimate end resistance and proposes an analytical equation to calculate the vertical ultimate compressive bearing capacity of monopiles in soft soil areas.

The advantage of the analytical equation proposed in this paper for calculating the vertical ultimate compressive bearing capacity of the monopile in soft soil area is that it can start from the perspective of transferring the load at the top of the pile along the pile body, consider the limitation of the ultimate pile lateral friction resistance, consider the influence of the pile's own gravity, coupled with the ultimate end resistance calculation method proposed by previous authors according to the deformation characteristics of the pile end, which makes the final monopile vertical ultimate bearing capacity prediction results more accurate.

As shown in Figure 1, in order to test the reliability of the prediction method in this paper, four engineering test piles in Suzhou, China, were chosen to carry out static load tests onsite. As a reliable bearing capacity detection method, the static load test can get the bearing capacity of single piles according to the characteristics of the load settlement curve, and the result is consistent with the predicted value. Finally, based on the field engineering situation, the finite element method simulates the loading process of four test piles, and the result is further compared with the data output by this prediction method from the aspects of deformation characteristics and structural stress. It is found that the deformation characteristics of the soil around the pile and the variation trend of the axial force along the pile shaft obtained by the simulation are consistent with the corresponding predicted results. In general, two research methods, static load test and numerical simulation, are chosen to corroborate the reliability of the newly proposed analytical equations for calculating the vertical ultimate compressive load capacity of monopiles in soft soil areas. The corroboration shows that the method proposed in this paper is a simple, economical, and accurate method for predicting the vertical ultimate compressive load capacity of monopiles in soft soil areas, which provides valuable experience for similar projects.

2. Calculation of Vertical Ultimate Compressive Bearing Capacity of Single Pile in Soft Soil Area

The approximate derivation line of the method is given as shown in Figure 2. The vertical ultimate compressive load capacity prediction method for monopiles proposed in this paper consists of two parts, one of which is the further derivation of the load transfer law in morphogenic soils based on Randolph's study on the internal forces of pile bodies in homogeneous soils, and the other part is Janbu's study on the ultimate end resistance of pile ends. In this paper, the two parts were linked and the analytical equations for the vertical ultimate compressive load capacity of a single pile were constructed.

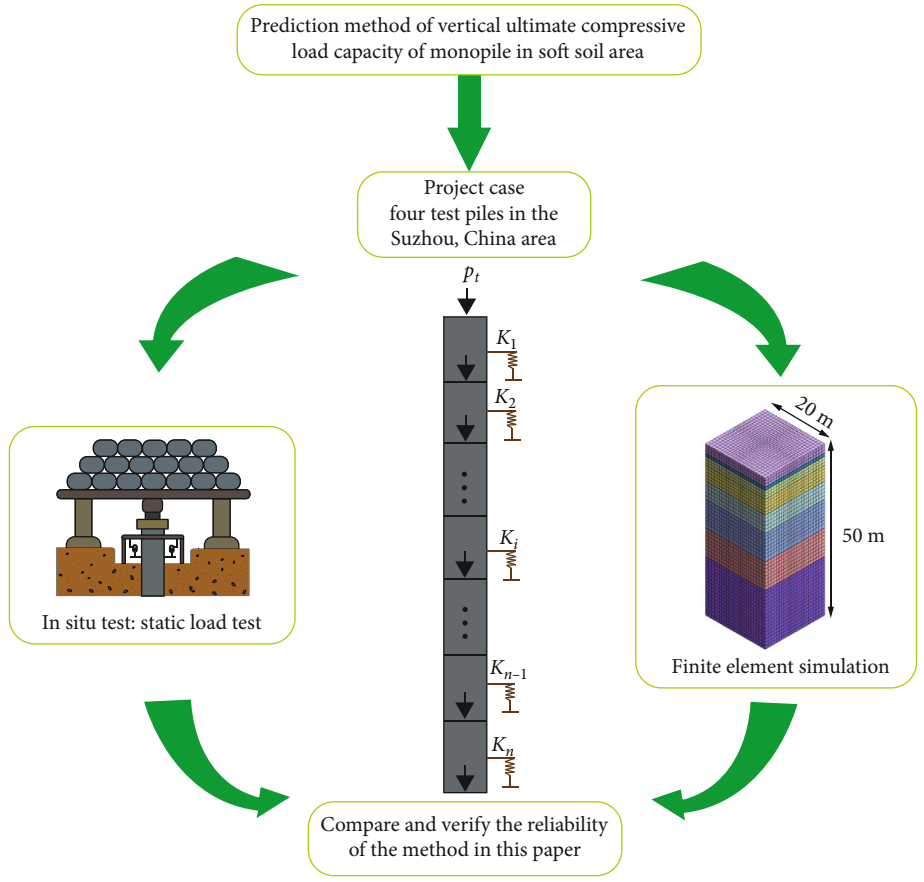

Figure 1: Proof route of the method in this paper.

2.1. Calculation of Pile Side Friction Resistance and Pile End Resistance in Layered Soils. In homogeneous soils, Randolph [41] proposed a method for calculating pile end resistance.

$$p_b = p_t \cdot \frac{(4\eta/((1-\nu_s)\xi))(1/\cosh(\mu L))}{(4\eta/((1-\nu_s)\xi)) + \rho(2\pi/\zeta)(\tanh(\mu L)/\mu L)(L/r_0)}. \quad (1)$$

Here,

$$\begin{aligned} \eta &= \frac{r_0}{r_b}, \\ \zeta &= \ln\left(\frac{r_m}{r_0}\right), \\ r_m &= 2.5\rho(1-\nu_s)L, \\ \rho &= \frac{G_{avg}}{G_L}, \\ \xi &= \frac{G_L}{G_b}, \\ G_L &= \frac{E_s}{2(1+\nu_s)}, \\ \mu L &= \sqrt{\frac{2G_L}{\zeta E_p}}\frac{L}{r_0}, \end{aligned} \quad (2)$$

where p_t is the load on the pile top, L is the pile length, r_m is the influence radius of the pile, r_0 is the radius of the pile, r_b is the radius of the pile end, ν_s is the Poisson's ratio of the soil layer, ρ is the soil inhomogeneity coefficient around the pile, G_{avg} is the average shear modulus within the pile length, G_L is the shear modulus of the soil at depth L, E_s is Young's modulus of the soil layer, G_b is the shear modulus of the soil at the pile end, and E_p is the elastic modulus of the pile.

For cylindrical piles, $\eta = 1$, $\rho = 1$, and $\xi = 1$. In this paper, considering the influence of the pile gravity G, Equation (1) can be further transformed into

$$p_b = (p_t + G) \cdot \frac{(4\eta/1-\nu_s)(1/\cosh(\mu L))}{(4\eta/(1-\nu_s)) + (2\pi/\zeta)(\tanh(\mu L)/\mu L)(L/r_0)}. \quad (3)$$

Thus, the pile side frictional resistance is calculated as follows.

$$p_s = p_t + G - p_b = (p_t + G) \cdot \frac{(4\eta/1-\nu_s)[1-(1/\cosh(\mu L))] + (2\pi/\zeta)(\tanh(\mu L)/\mu L)(L/r_0)}{(4\eta/1-\nu_s) + (2\pi/\zeta)(\tanh(\mu L)/\mu L)(L/r_0)}. \quad (4)$$

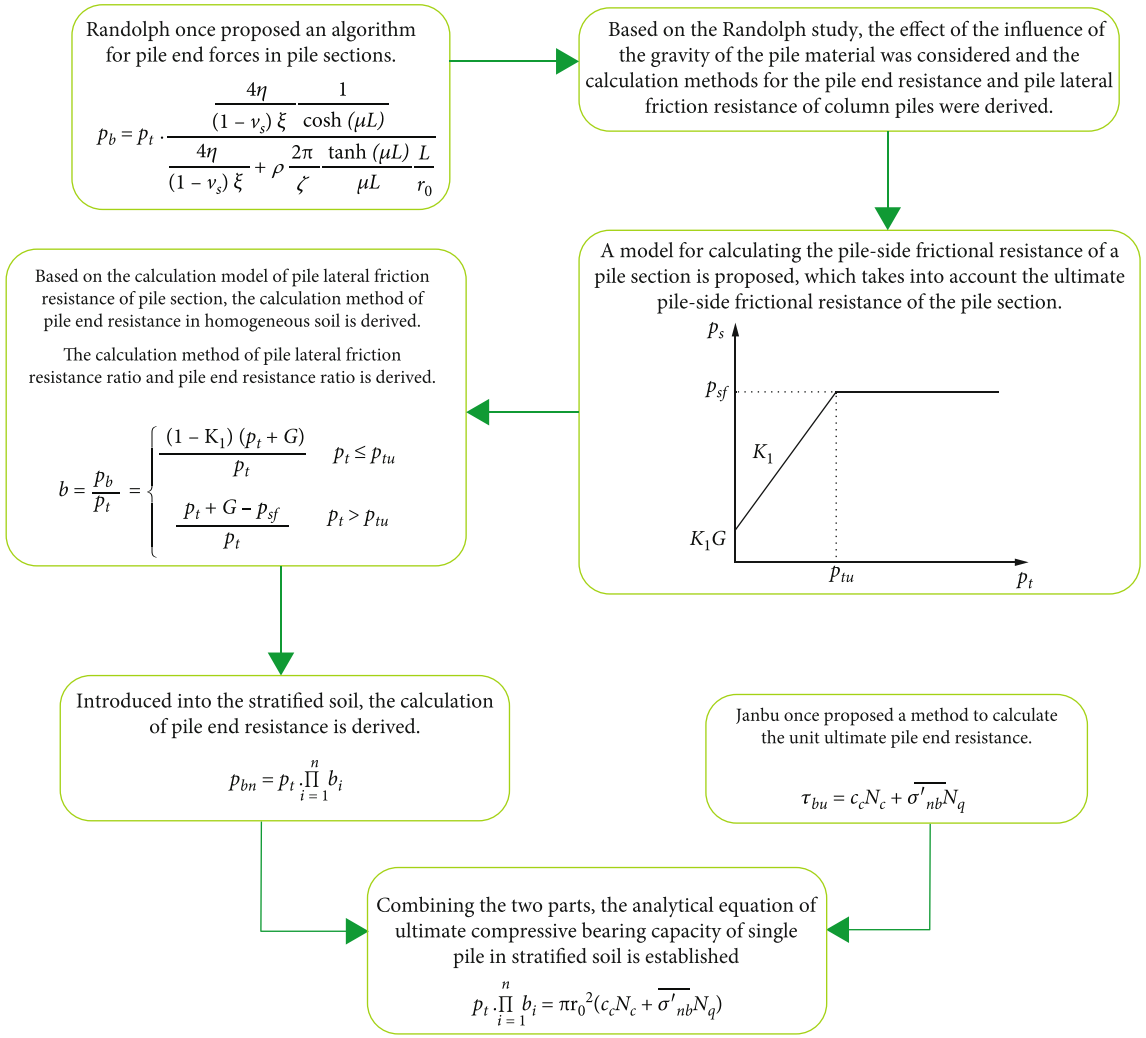

Figure 2: Derivation route of the calculation method.

The pile side frictional resistance increases with the load on the pile top but is limited by the ultimate pile side frictional resistance. In Equation (4), the limit of pile side ultimate frictional resistance is not taken into account, which will be considered and corrected in the next part of this paper.

In this paper, the calculation model of the ideal elastoplastic double fold line is selected to describe the relationship between the unit pile lateral frictional resistance and the relative displacement of the pile and soil, as shown below.

$$\tau = \begin{cases} C_S S & S \le S_u, \\ \tau_{su} & S > S_u, \end{cases} \quad (5)$$

where τ is the pile side friction resistance per unit length at the relative displacement, C_s is the body shear deformation parameter, S is the pile-soil relative displacement, S_u is the ultimate elastic displacement of the soil around the pile, τ_{su} is the ultimate pile side friction resistance. The calculation model is shown in Figure 3.

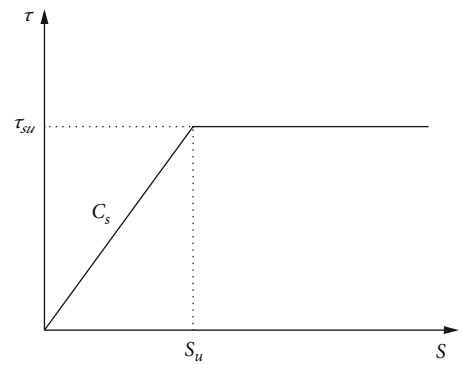

Figure 3: Calculation model of the ideal elastoplastic double fold line.

According to the previous research [31], the unit limit pile lateral friction resistance can be calculated using the following equation.

$$\tau_{su} = K_0\left(\frac{K}{K_0}\right)\tan\left[\varphi\left(\frac{\delta}{\varphi}\right)\right]\sigma'_v = K_0\left(\frac{K}{K_0}\right)\tan\left[\varphi\left(\frac{\delta}{\varphi}\right)\right]\gamma h, \quad (6)$$

Table 1: The recommended value of δ.

Engineering status	δ	Derived from
Smooth concrete piles	$(0.8 \sim 1.0)\varphi$	Kulhawy [42]
Concrete pile, clay, and silt	$21.3^\circ \sim 31.6^\circ$	Liu and Zhu [44]
Smooth H-piles steel or pipe piles	$(0.5 \sim 0.7)\varphi$	Kulhawy [42]
Pipe pile, dense sand	29.4°	O'Neill and Raines [45]
Driven pile, sand	$28^\circ \sim 30^\circ$	Jardine [46]

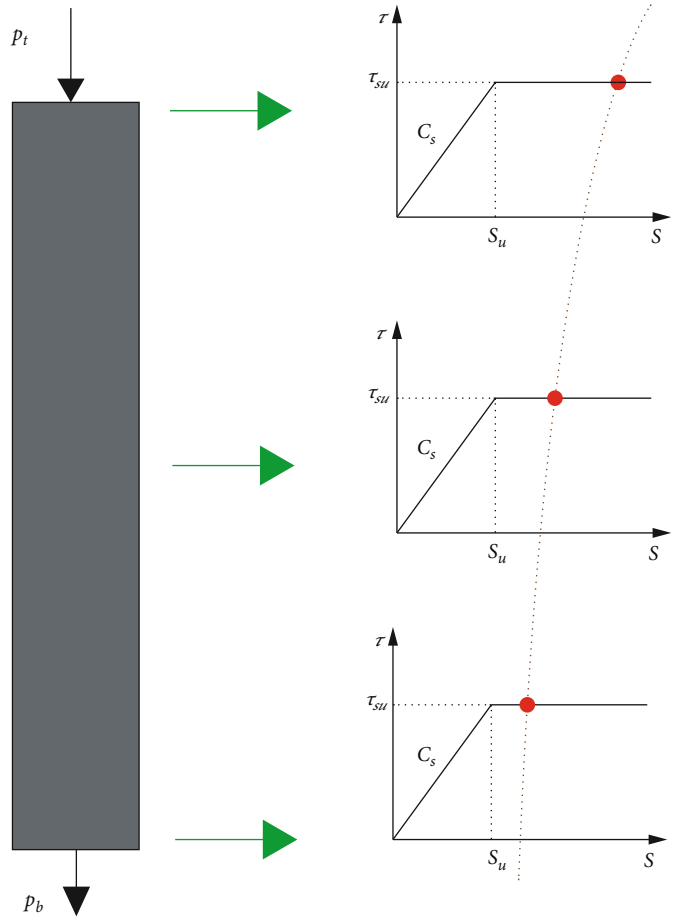

Figure 4: Ultimate pile side friction resistance per unit length at each point in the pile section.

where K is the lateral pressure coefficient; K_0 is the in situ earth pressure coefficient, and it can be estimated through the equation $K_0 = 1 - \sin\varphi$; δ is the friction angle at the pile-soil interface; φ is the effective internal friction angle of the soil on the pile side; δ_v' is the effective overburden weight at a given depth; γ is the soil capacity. As for the value of K, Kulhawy [42] suggested that the value of K/K_0 should be in the range of 0.7 to 1.2 for smooth H-shaped piles, steel pipe piles, and small displacement concrete piles. For smooth H-shaped piles, steel pipe piles, and large displacement concrete piles, the value of K/K_0 should be in the range of 1 to 2.

Some researchers have summarized the suggested values of δ [43], as shown in Table 1.

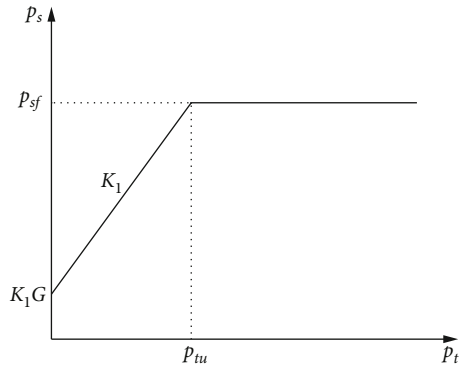

Figure 5: Calculation model of pile side friction resistance of pile section.

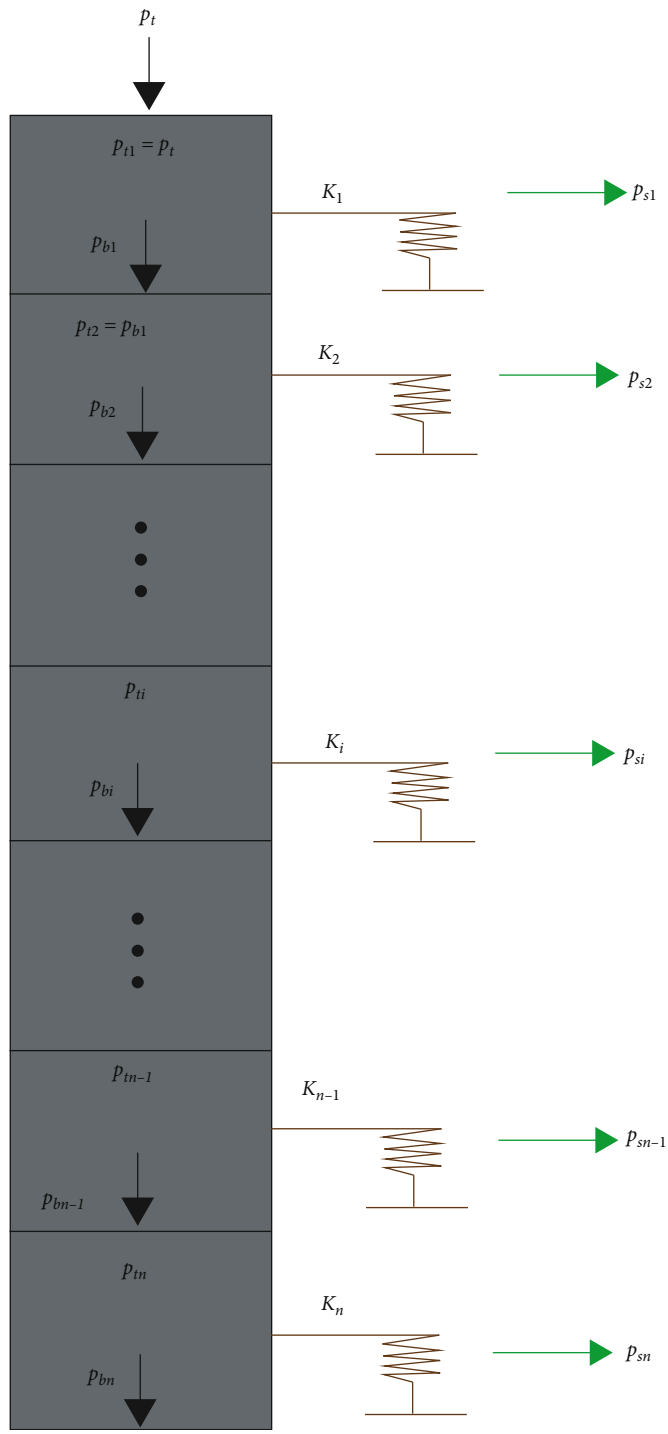

Figure 6: Load transfer schematic.

Regarding δ, another calculation method is given by researchers as follows [47]:

$$\delta = \arctan\left[\frac{\sin\varphi\cos\varphi}{1+\sin^2\varphi}\right]. \tag{7}$$

In homogeneous soils, when the pile segment is subjected to the ultimate pile side frictional resistance, as shown in Figure 4, the pile side frictional resistance per unit length of the pile segment has also reached the ultimate value.

Therefore, for a pile segment, the ultimate pile side friction resistance is

$$p_{sf} = 2\pi r_0 \int_{h1}^{h2} \tau_{su} d(h) = 2\pi r_0 K_0 \left(\frac{K}{K_0}\right) \tan\left[\varphi\left(\frac{\delta}{\varphi}\right)\right] \int_{h1}^{h2} \gamma h d(h), \tag{8}$$

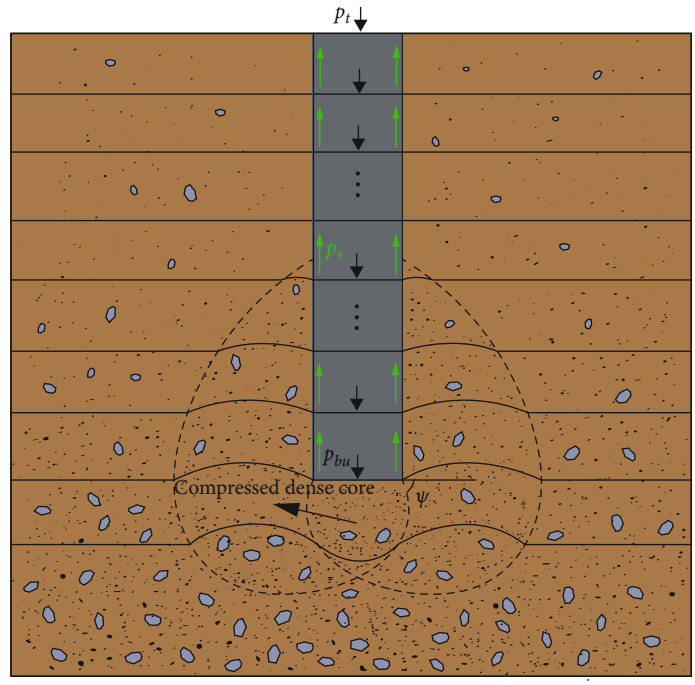

Figure 7: Pile end damage pattern.

Table 2: Soil layer parameters of 4 test piles.

Number	Name of soil layer	Thickness (m)				ν_s	c_c	$\varphi(\circ)$	$\gamma(\mathrm{kN/m^3})$	E_s(kpa)
		TS1	TS2	TS4	TS3					
1	Plain fill 1	2.63	3.82	2.55	0	0.18	18	12.3	18.7	54600
2	Plain fill 2	0	0	0	2.61	0.375	12	10	18.92	36360
3	Silty clay 1	1	2.2	2.2	0	0.37	31	13.7	19	68850
4	Muddy silty clay 1	2.6	2.2	2.3	0	0.42	10	8.6	17.7	34950
5	Muddy silty clay 2	0	0	0	4	0.394	10	16.1	19.06	23100
6	Silty clay 2	4.6	4.6	4.2	0	0.31	25	15.4	18.8	73050
7	Silty clay 3	0	0	0	3	0.310	24.3	16	19.14	39780
8	Silt mixed with silt 1	0	0	0	4.6	0.281	7	23.8	19.21	46260
9	Silt mixed with silt 2	0	0	0	7.9	0.254	4	30.9	19.62	52500
10	Silty sand, mixed with silt	5.3	5.3	6.48	0	0.28	4	29.6	19.2	149700
11	Muddy silty clay 3	0	0	0	6.89	0.329	24.9	14.9	18.4	28200
12	Clay	7.07	6.98	7.62	0	0.25	59	13.2	20.1	130200
13	Silty clay, intercalated clay	0	0	4.65	0	0.28	42.3	14	19.7	113550

where h_1 is the starting height of the pile section; h_2 is the ending height of the pile section. Let

$$K_1 = \frac{(4\eta/(1-\nu_s))[1-(1/\cosh(\mu L))] + (2\pi/\zeta)(\tanh(\mu L)/\mu L)(L/r_0)}{(4\eta/(1-\nu_s)) + (2\pi/\zeta)(\tanh(\mu L)/\mu L)(L/r_0)}. \tag{9}$$

After considering the limit pile side friction resistance limit in the pile section, then the modified pile side friction of this paper is calculated as follows.

$$p_s = \begin{cases} K_1(p_t + G) & p_t \le p_{tu}, \\ p_{sf} & p_t > p_{tu}, \end{cases} \tag{10}$$

where p_{tu} is the load on the pile top corresponding to the limit of pile side friction resistance, and its value can be back-calculated from Equation (4), i.e.: $p_{tu} = (p_{sf}/K_1) - G$. The model for calculating the pile side friction resistance of the pile section is shown in Figure 5.

Table 3: Pile end parameters.

Pile number	Soil at the end of the pile	Pile length (m)	c_c	$\psi(\circ)$	N_c	$\overline{\sigma'_{nb}}$	N_q	p_{bu}(kN)
TS1	Clay	23.2	59	70	7.775	376.873	2.834	430.575
TS2	Clay	25	59	70	7.775	406.031	2.824	453.854
TS3	Muddy silty clay 3	29	24.9	70	8.426	458.354	3.242	479.492
TS4	Silty clay, intercalated clay	30	42.3	70	8.073	485.063	3.013	509.743

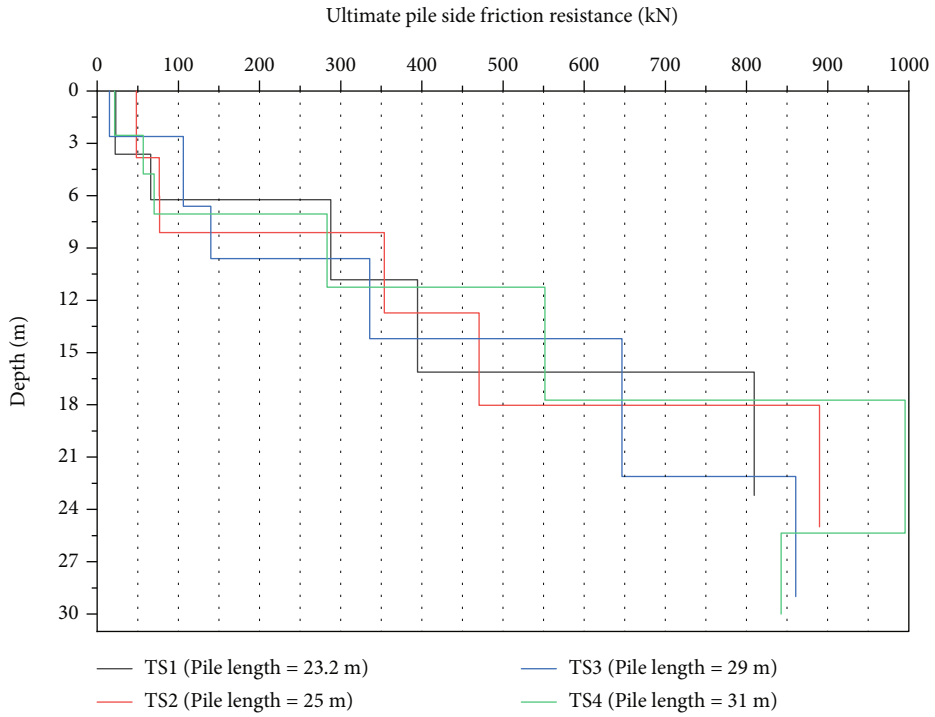

Figure 8: Ultimate pile side friction resistance of pile section.

Therefore, the pile side friction resistance ratio of this pile section is

$$a = \frac{p_s}{p_t} = \begin{cases} (K_1(p_t + G)/p_t) & p_t \le p_{tu} \\ p_{sf}/p_t & p_t > p_{tu} \end{cases} \quad (11)$$

The pile end resistance of the pile section after correction in this paper is

$$p_b = p_t + G - p_s = \begin{cases} (1 - K_1)(p_t + G) & p_t \le p_{tu} \\ p_t + G - p_{sf} & p_t > p_{tu} \end{cases} \quad (12)$$

Thus, the pile end resistance ratio of this pile section is

$$b = \frac{p_b}{p_t} = \begin{cases} ((1 - K_1)(p_t + G)/p_t) & p_t \le p_{tu} \\ \left(p_t + G - p_{sf}/p_t\right) & p_t > p_{tu} \end{cases} \quad (13)$$

In this paper, the method is introduced to the layered soil, and the pile in each layer of soil is regarded as a new pile segment, so the pile end resistance of the pile segment in the previous layer is regarded as the axial force there and also the load on the pile top of the next layer. The load transfer schematic is shown in Figure 6.

As shown in Figure 6, p_{ti} is the load on pile section i; p_{si} is the pile side friction of pile section i; p_{bi} is the pile end force of pile section i. Assuming that the pile corresponds to a soil layer with n layers, after n transfers of the pile top load along the pile body, the pile end resistance obtained is

$$p_{bn} = p_t \cdot \prod_{i=1}^{n} b_i \quad (14)$$

where b_i is the pile end resistance ratio of pile section i.

2.2. Ultimate Pile End Resistance. Janbu [40] proposed a calculation method for unit ultimate end resistance based on the ball hole expansion theory.

$$\tau_{bu} = c_c N_c + \overline{\sigma'_{nb}} N_q \quad (15)$$

where c_c is the cohesion force of the soil at the pile end; $\overline{\sigma'_{nb}}$ is the average effective pressure on the lateral side at the pile

Table 4: Load transfer data from top to bottom along the pile.

Name of soil layer	Undamaged test piles			Damaged test pile
	TS1	TS2	TS4	TS3
Pile top load (kN)	1856.337	2179.249	3102.119	2362.212
Axial force (b_1)	1853.493 (0.998)	2160.054 (0.991)	3100.038 (0.999)	2367.140 (1.002)
Axial force (b_2)	1839.057 (0.992)	2100.448 (0.972)	3060.083 (0.987)	2291.510 (0.968)
Axial force (b_3)	1792.943 (0.974)	2039.467 (0.971)	3007.357 (0.983)	2174.308 (0.949)
Axial force (b_4)	1540.321 (0.859)	1720.680 (0.844)	2756.288 (0.917)	1873.606 (0.862)
Axial force (b_5)	1186.001 (0.770)	1290.531 (0.750)	2254.137 (0.818)	1287.498 (0.687)
Axial force (b_6)	430.576 (0.363)	453.854 (0.352)	1316.916 (0.584)	479.491 (0.372)
Axial force (b_7)			509.741 (0.387)	
Ultimate pile end resistance (kN)	430.576	453.854	509.741	479.491

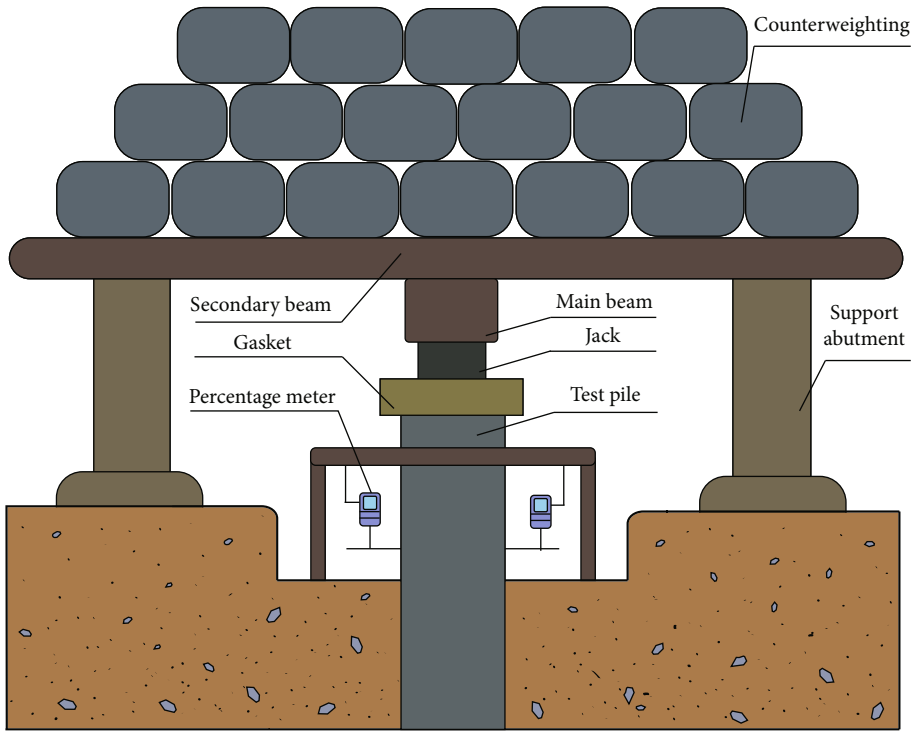

Figure 9: Field static load test device schematic diagram.

end plane. As described by researchers [48], N_c and N_q are the dimensionless bearing capacity coefficients that reflect the cohesive force of the soil and the effect of lateral earth pressure at the pile end plane, respectively. They can be calculated by the following method.

$$N_c = \left(N_q - 1\right) \cot \varphi,$$
$$N_q = \left(\tan \varphi + \sqrt{1 + \tan^2 \varphi}\right)^2 e^{2\psi \tan \varphi}, \quad (16)$$
$$\overline{\sigma'_{nb}} = \frac{1 + 2K_0}{3} \sigma'_{vb},$$

where σ'_{vb} is the effective vertical stress at the pile end; ψ is the angle between the pile end compaction core boundary

Table 5: Graded loading value of pile top load for each test pile.

Number of levels	Pile top load (kN)			
	TS1	TS2	TS3	TS4
1	350	420	480	540
2	525	630	720	810
3	700	840	960	1080
4	875	1050	1200	1350
5	1050	1260	1440	1620
6	1225	1470	1680	1890
7	1400	1680	1920	2160
8	1575	1890	2160	2430
9	1750	2100	2400	2700

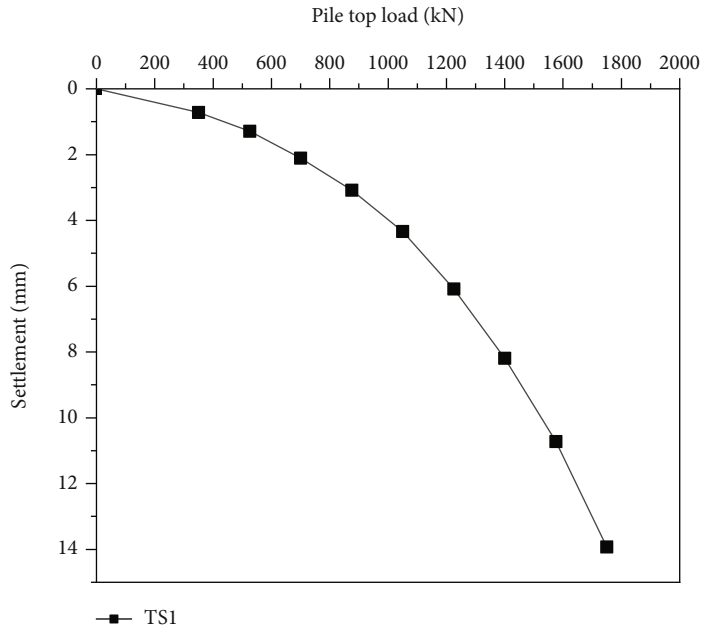

(a)

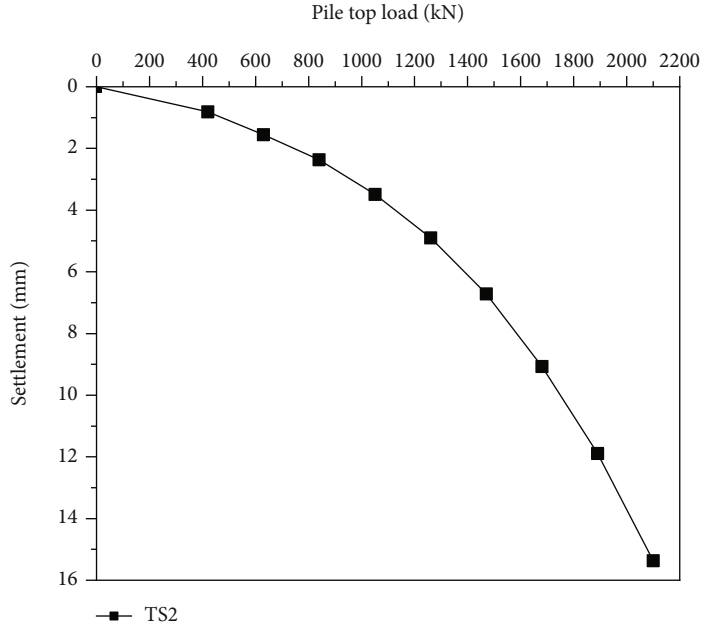

(b)

Figure 10: Continued.

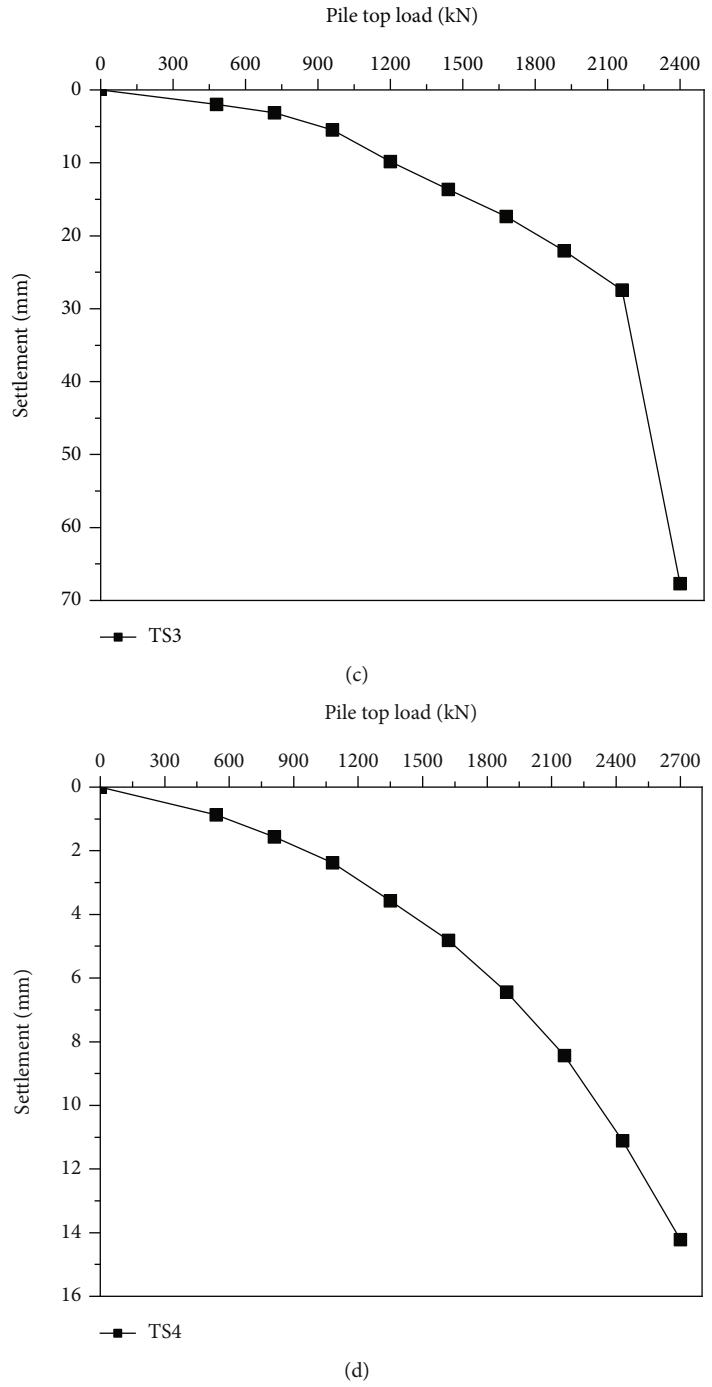

Figure 10: Static load test results. (a) TS1; (b) TS2; (c) TS3; (d) TS4.

and the horizontal plane in the failure mode of pile end soil. The compressibility of soil can be determined by in situ testing methods such as penetration tests. Generally, it is about 60^0 for soft clay and about 105^0 for dense sandy soil [48].

Combined with the above discussion, the ultimate pile end resistance calculation method derived in this paper is as follows:

$$p_{bu} = \pi {r_0}^2 \tau_{bu} = \pi {r_0}^2 \left(c_c N_c + \overline{\sigma'_{nb}} N_q \right). \tag{17}$$

2.3. Analytical Equation of Vertical Ultimate Compressive Load Capacity of Single Pile. The load on the top of the pile is transmitted downward from the pile body to the pile end. When the pile end resistance reaches the ultimate value, the pile end will occur sliding shear failure, and its shape is shown in Figure 7. At this time, the load on the pile top is the ultimate bearing capacity of a single pile.

Combining Equation (14) and Equation (17), the analytical equation for the vertical ultimate compressive bearing

Table 6: Comparison of vertical ultimate compressive load bearing capacity results.

Pile number	Whether to damage	Last load value (kN)	Maximum load value (kN)	Vertical ultimate compressive load capacity (kN)	
				Static load test result	Calculation results
TS1	No	1575	1750	1750	1856.337
TS2	No	1890	2100	2100	2179.249
TS3	Yes	2160	2400	2160	2362.212
TS4	No	2430	2700	2700	3102.119

capacity of a single pile in a layered soil is established as follows.

$$p_t \cdot \prod_{i=1}^{n} b_i = \pi {r_0}^2 \left(c_c N_c + \overline{\sigma'_{nb}} N_q \right). \tag{18}$$

For load p_t, if there is a corresponding pile end resistance ratio b_1, ..., b_n of each pile section, making Equation (18) tenable, the solution of the equation is the vertical ultimate compressive bearing capacity of a single pile.

3. Application of Engineering Cases

In this paper, four engineering test piles with different lengths, TS1, TS2, TS3, and TS4, were selected for the application of the method in the soft soil area of Suzhou, China; among them, TS1, TS2, and TS4 were nondestructible test piles,while TS3 was a destructible test pile. The type of pile is the bored pile. The design strength grade of concrete is submerged C30. the diameter of all four test piles is 0.6 m. As shown in Table 2, the calculated parameters of each soil layer in this paper are extracted from the engineering geological survey report and summarized as follows: among them, Poisson's ratio v_s, cohesion c_c, and internal friction angle φ of the soil can be measured by triaxial tests; the density γ and elastic modulus E_s of the soil can be measured by indoor geotechnical tests.

The calculated parameters of the pile end for the four test piles are summarized in Table 3. Among them, the value of ψ, since the soil at the pile end consists mainly of clay, as suggested by Zhang [48], is 70 degrees as taken in this paper.

The data in the table were substituted into the proposed method to predict the bearing capacity of four engineering test piles. Among them, the ultimate pile side friction resistance p_{sf} of each pile section is shown in Figure 8. The magnitude of the vertical line represents the limit of frictional resistance that can be achieved for each pile segment at each depth. From the trend of the graph line, it is indicated that the ultimate pile side friction resistance will increase with the increase of depth, and the changing trend is the same for each test pile.

The final bearing capacities of test piles TS1, TS2, TS3, and TS4 calculated by this method are 1856.337 kN, 2179.249 kN, 2362.212 kN, and 3102.119 kN, respectively. When the test piles are subjected to ultimate compressive bearing capacity, the bottom axial force and pile end resistance of each soil layer from top to bottom are shown in Table 4.

4. Single Pile Static Load Test

In order to test the reliability of the method in this paper, static load tests were conducted in the field on the four engineering test piles mentioned above. The installation of the field static load test is shown in Figure 9.

4.1. Testing Method. The test method of the vertical ultimate compressive bearing capacity of the test piles in this project adopts the slow maintenance load method. Testing was based on the technical code for testing of building foundation piles [49]. The reaction force of the load adopted the reaction force device of the deadweight platform, and the stack load required to be applied to the deadweight platform is not less than 1.2 times the maximum load value of the pile top load. The graded loading value of the pile top load of each test pile is shown in Table 5.

4.1.1. Reading Method. After each level of load was applied to the pile top, readings of pile top settlement were taken at the 5th, 15th, 30th, 45th, and 60th minutes. Thereafter, pile top settlement readings were taken at 30-minute intervals.

4.1.2. Judgment Criteria for Settlement Stability. The settlement stability is judged by the following criterion: under each level of load, the settlement of the pile top is found to be no more than 0.1 mm per hour in two consecutive tests. When the settlement rate of the pile top reaches the relative stability criterion, then the next level of load is applied.

4.1.3. Conditions for Termination of Loading. The technical code for testing of building foundation piles stipulates the following five conditions for termination of loading [49]:

(1) Under a certain level of loading, if the settlement at the top of the pile is greater than 5 times the settlement under the previous level of loading and the total settlement at the top of the pile exceeds 40 mm, the loading should be terminated

(2) Under a certain level of loading, if the settlement at the top of the pile is greater than two times the settlement under the previous level of loading, and the standard of settlement stability has not been reached after 24 hours, the loading should be terminated

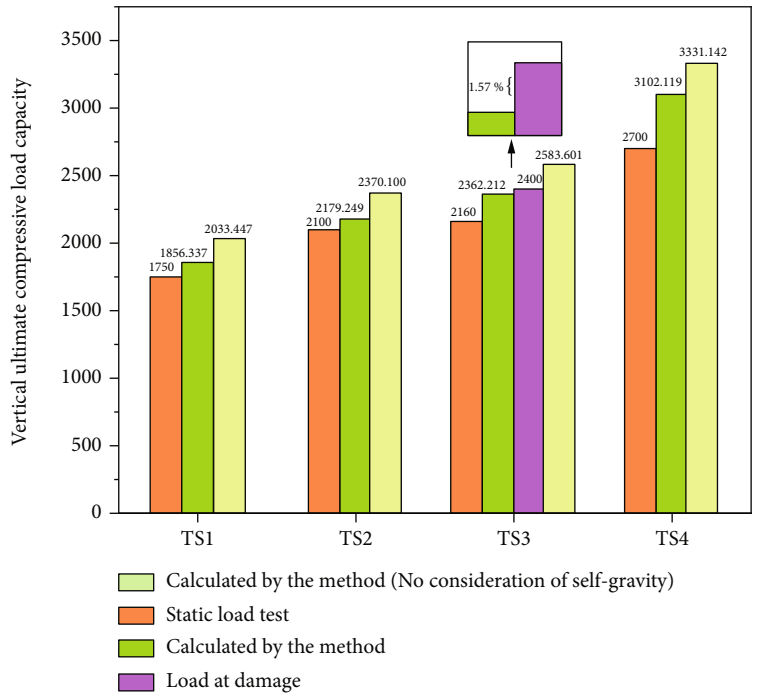

Figure 11: Vertical ultimate compressive load capacity of each test pile.

(3) If the pile top load loading value has reached the maximum loading value required by design and the pile top settlement has reached the standard of settlement stability

(4) If the anchor pile is used as an anchor pile, the loading should be terminated if the anchor pile has reached the permitted value

(5) When the load-settlement curve is slowly changing, it can be loaded until the total settlement at the top of the pile is 60 mm~80 mm; when the resistance at the end of the pile is not fully developed, it can be loaded until the cumulative settlement at the top of the pile is more than 80 mm

4.2. Analysis of Results. The load-settlement curves obtained from the static load test are shown in Figure 10. It can be seen that the curves corresponding to TS1, TS2, and TS4 belong to slow deformation, while that of TS3 belongs to steep settlement type. According to the technical code for testing of building foundation piles [49], the loading load on TS1, TS2, and TS4 test piles should be terminated when the designed maximum loading is reached and the settlement of the pile top meets the standard of relative stability. For TS3, when the load reaches the maximum loading value of 2400 kN, the load-settlement curve shows obvious steep drop characteristics, which means that the test pile has been damaged. Therefore, the vertical ultimate compressive bearing capacity of the TS3 test pile should be taken as the loading value of the previous test pile without damage, i.e., the load value corresponding to the starting point of an obvious steep drop, which is 2160 kN.

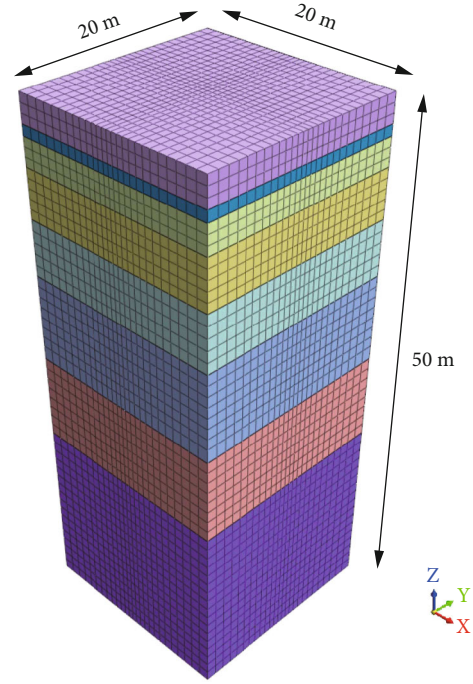

Figure 12: Finite element model diagram.

Table 6 summarizes the vertical ultimate compressive load bearing capacity obtained from the static load test and the prediction method of this paper. From the comparison of the results, the predicted ultimate bearing capacity of the static load test is conservative, while the pile actually does not reach the ultimate bearing state at this time. Therefore, in theory, the results calculated by the method in this paper should be greater than the results of the static load

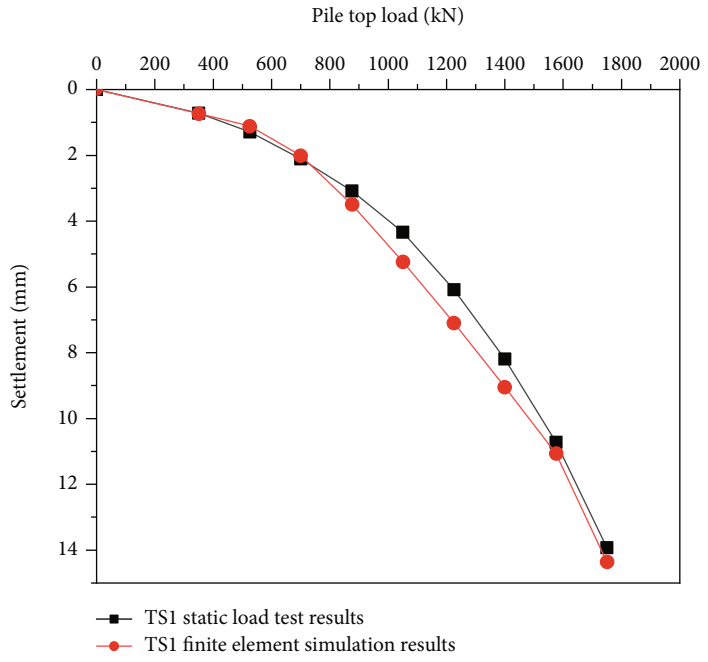

(a)

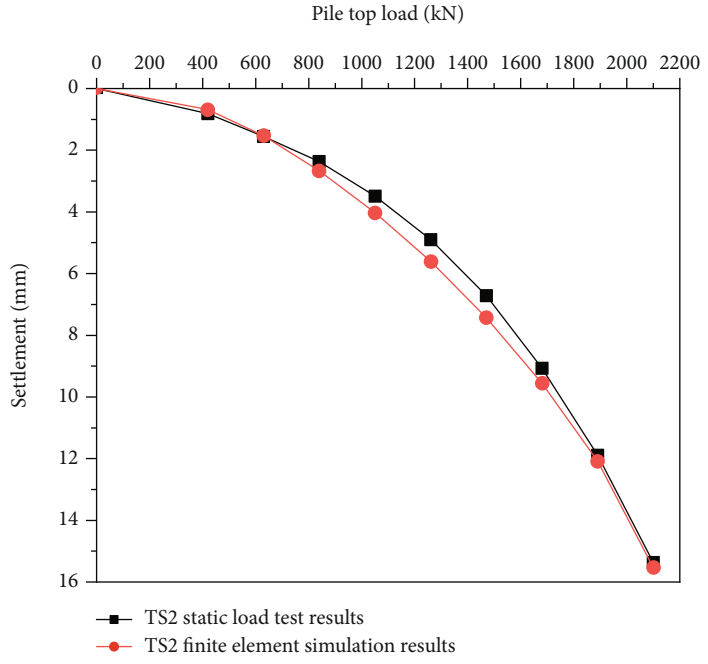

(b)

Figure 13: Continued.

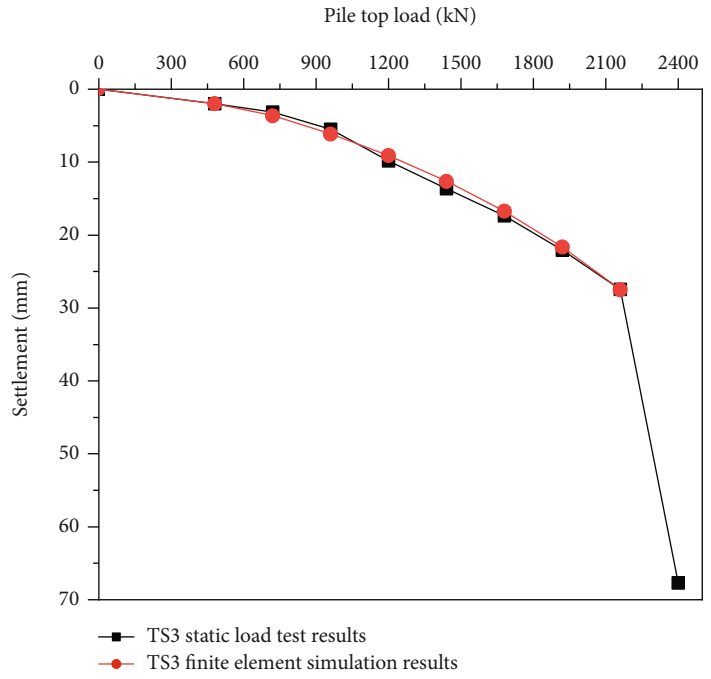

(c)

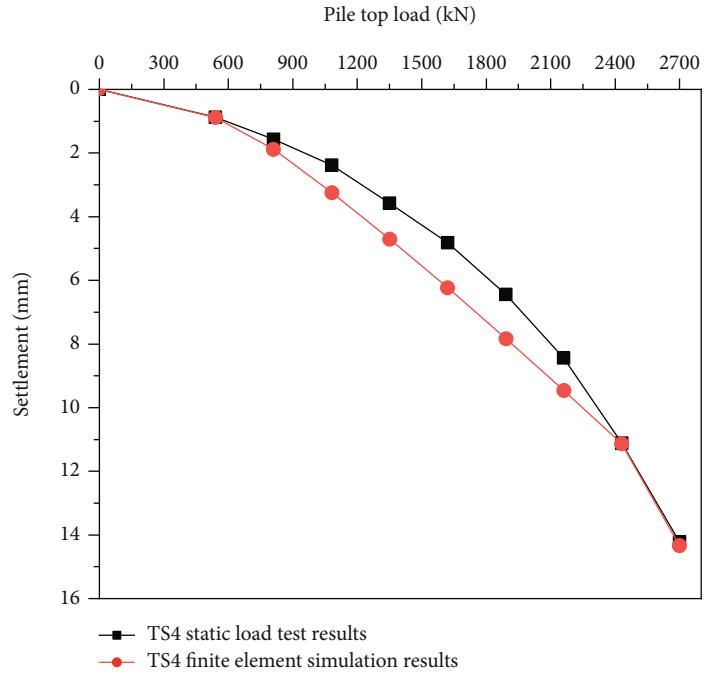

(d)

Figure 13: Load-settlement curve. (a) TS1; (b) TS2; (c) TS3; (d) TS4.

test, which is also fully reflected in the table. Further analysis of the data shows that the difference between the vertical ultimate compressive load capacity obtained from the static load test and the method in this paper is not much, which fully demonstrates the high accuracy of the calculation method. In addition, it is also obtained that the longer the length of the pile, the stronger the law of its vertical ultimate compressive load capacity. Therefore, the results of the field static load tests of TS1, TS2, TS3, and TS4 can coincide with the results of the method in this paper.

As shown in Figure 11, this paper also incorporated the comparison of the results of the method without considering the effect of the pile's own gravity. It can be clearly observed from the Figure 11 that the vertical ultimate compressive load bearing capacity results obtained by the method without considering the effect of the pile's self-gravity are

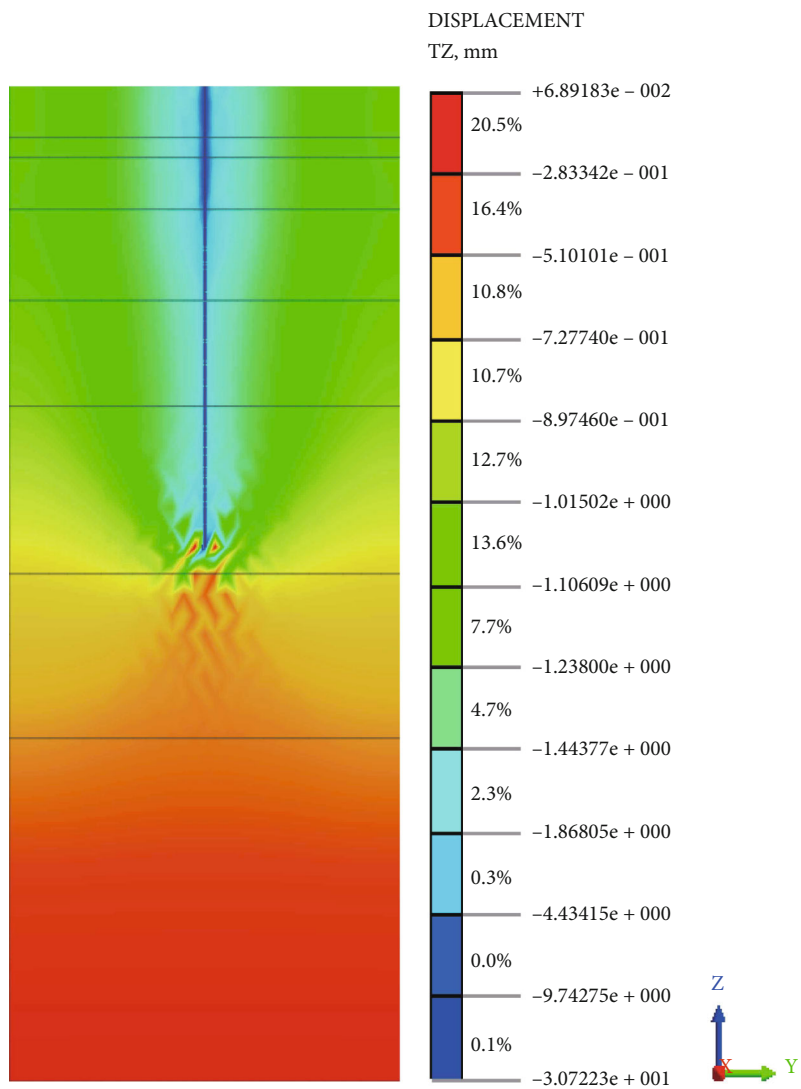

(a)

Figure 14: Continued.

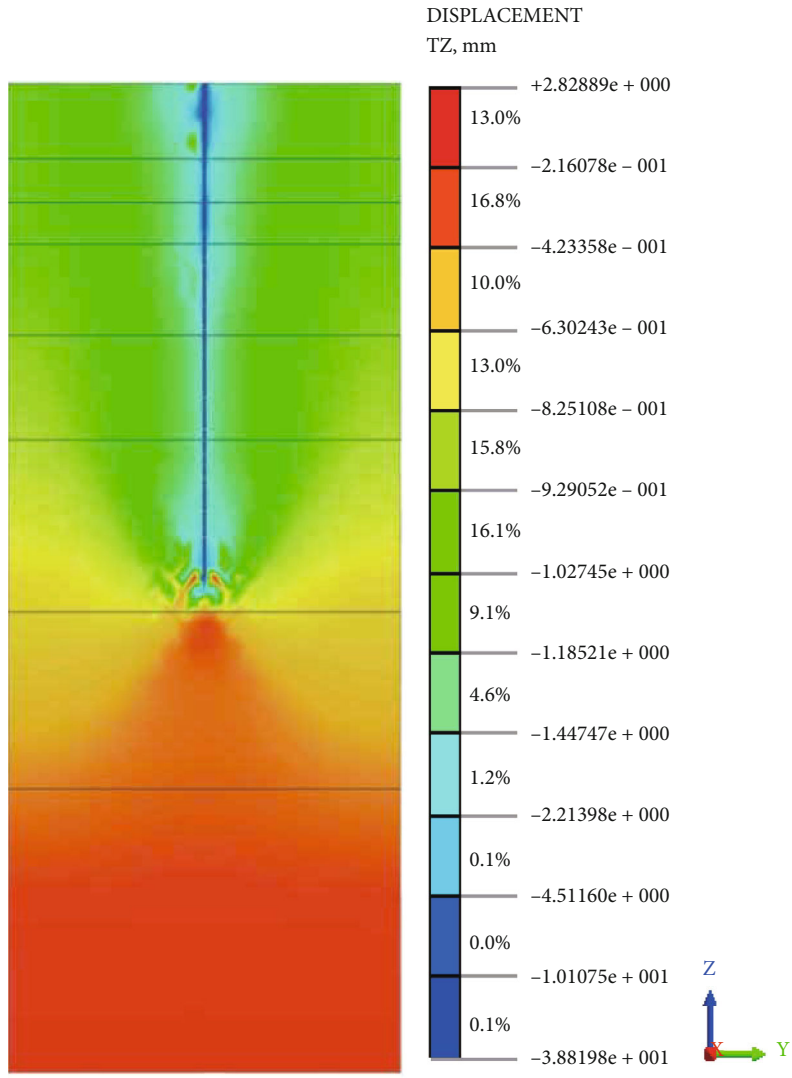

(b)

Figure 14: Continued.

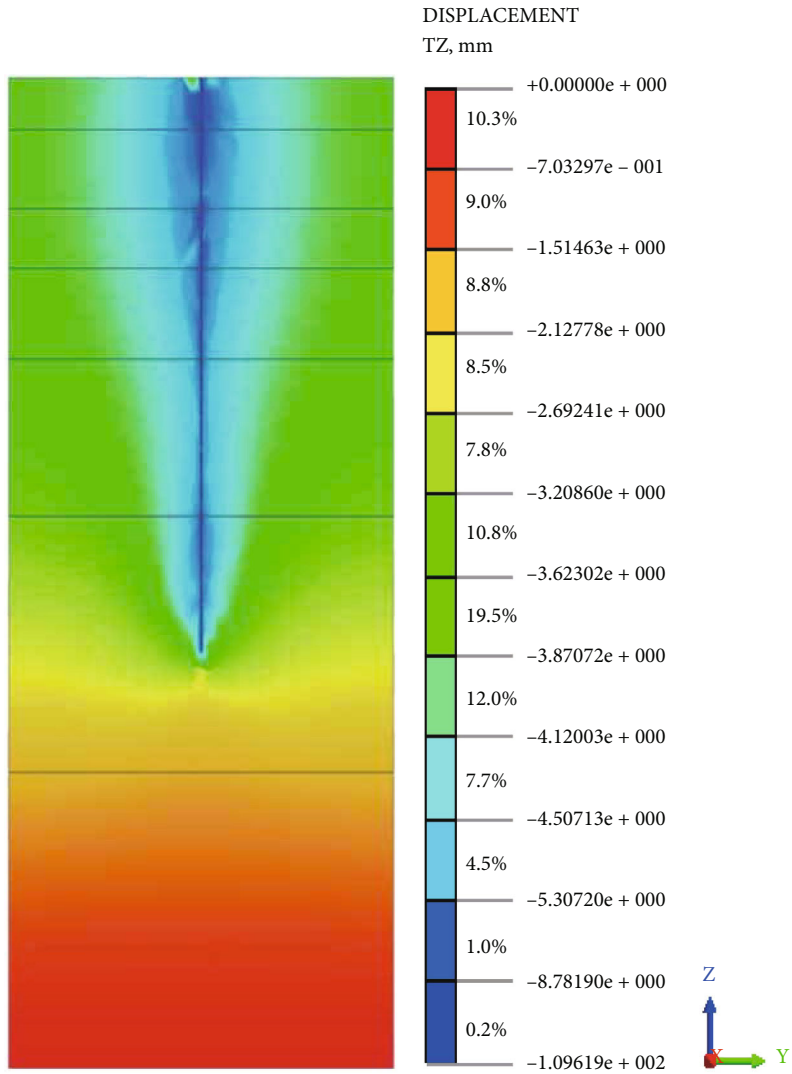

(c)

Figure 14: Continued.

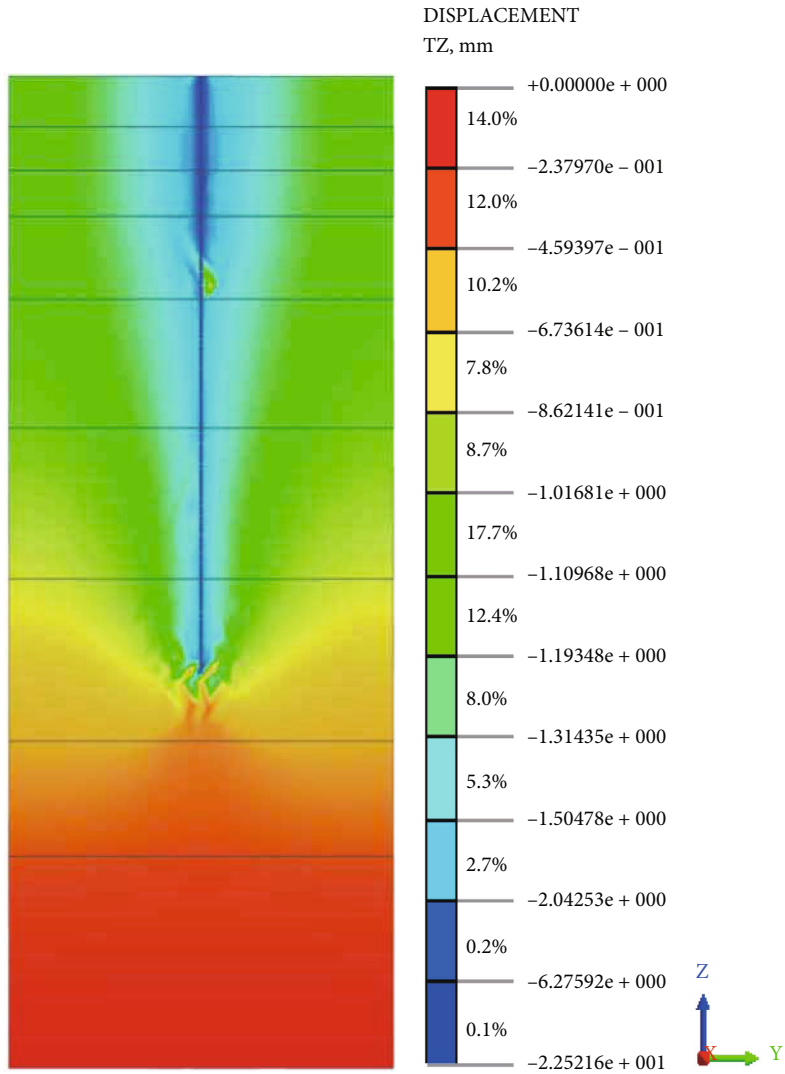

(d)

Figure 14: Settlement deformation diagram in the z-direction. (a) TS1, pile top load of 1750 kN; (b) TS2, pile top load of 2100 kN; (c) TS3, pile top load of 2160 kN; (d) TS4, pile top load of 2700 kN.

generally larger than considering its self-gravity, which is more obvious compared with the results of static load test detection, which greatly increases the error of prediction results. Therefore, it is a necessity to consider the pile's self-gravity to calculate the vertical ultimate compressive load-bearing capacity.

In addition, the static load test results contain both the damaged engineering test piles, including undamaged test piles, which are more valuable for comparison. If the results of the damaged test piles are used to evaluate the accuracy of the calculation results in the static load test, the loading value of the TS3 test pile is 2400 kN, and the vertical ultimate compressive bearing capacity calculated by the proposed is 2362.212 kN, the error rate between them is very small, roughly estimated to be only 1.57%. Therefore, the prediction method of the vertical ultimate compressive load capacity for single pile in soft soil area proposed in this paper is an excellent method.

5. Finite Element Simulation of Test Pile Loading Process

In order to further test the reliability of the prediction method, the finite element simulation of the loading process was carried out for four test piles with the same dimensions of 20 m in length, 20 m in width, and 50 m in height. The pile material ontology model adopts the elastic model, considering the pile concrete material is submerged C30, its elastic modulus is taken as 30 Gpa, its capacitance is 27 kN/m^3 and Poisson's ratio is 0.16. The soil ontology relationship adopts the Mohr-Coulomb model. The soil material parameters defined by the model include soil thickness, soil Poisson's ratio, soil cohesion, angle of internal friction, soil gravity, and soil modulus of elasticity from Table 2. The model should be empirically set up for the contact interface between pile and soil, and the interface can well simulate the relationship between pile lateral resistance and relative

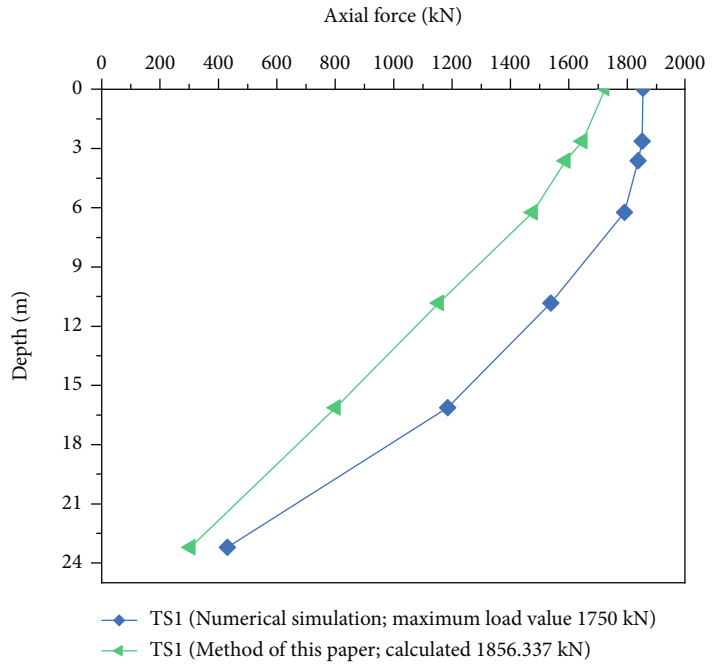

(a)

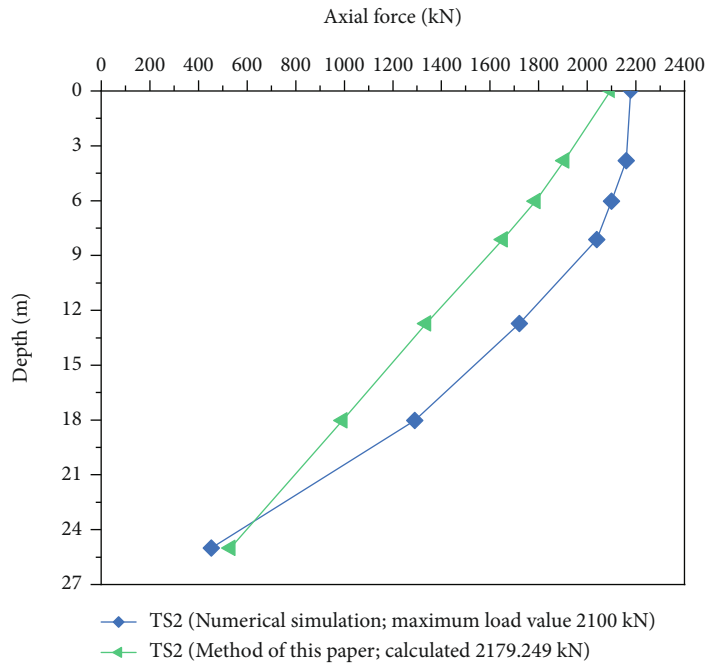

(b)

Figure 15: Continued.

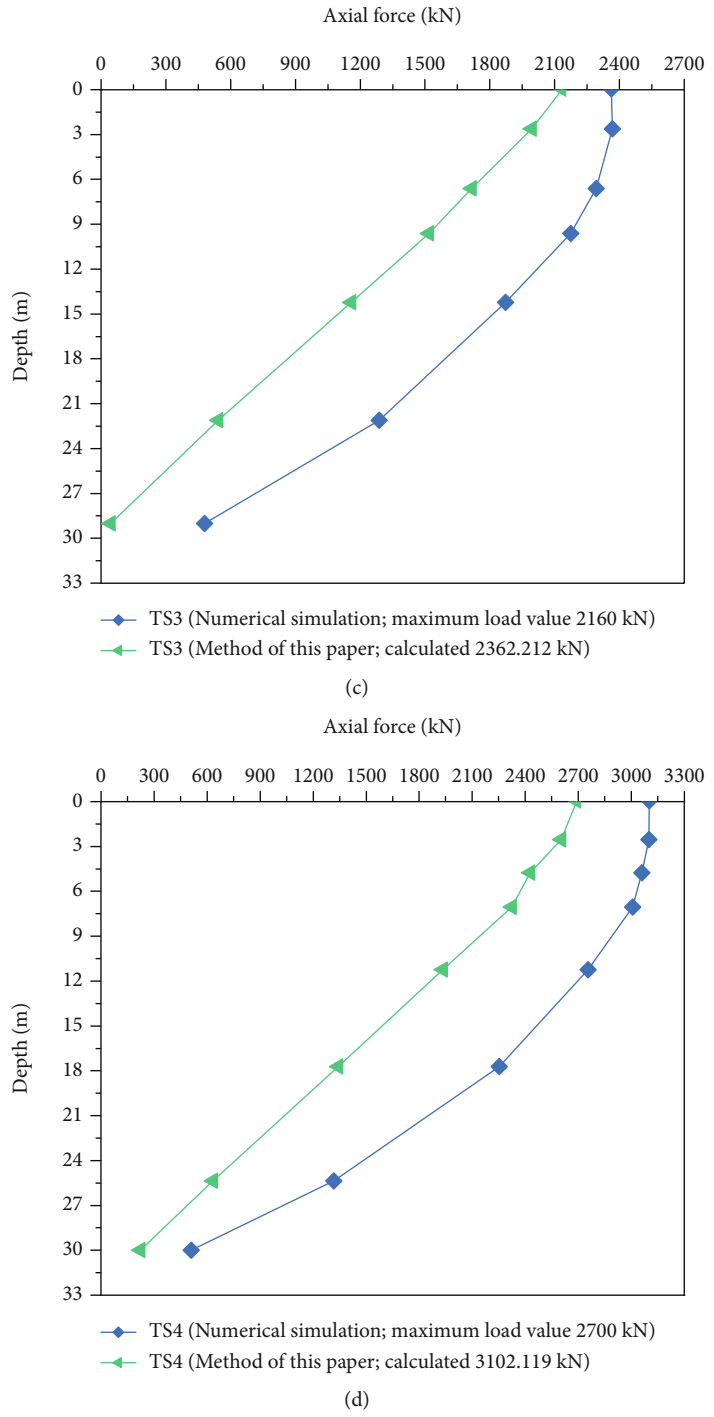

Figure 15: Axial force distribution of each test pile under the given conditions.

displacement through the embedded displacement-friction function. The model has fixed X-directional constraints on the left and right, fixed Y-directional constraints on the front and back, and three fixed XYZ constraints on the bottom. The finite element simulation considered the effect of the gravity field, and the simulation process was divided into three stages, including the initial stress stage, piling stage, and loading stage. In order to fit the loading process of the static load test to the greatest extent, the displacements of the first two stages are cleared to zero. The finite element model is shown in Figure 12.

As can be seen from Figure 13, the settlements of TS1, TS2, TS3, and TS4 obtained from the finite element simulation under all levels of pile top loading do not differ much from the settlements obtained from the static load test. On the whole, the results of the finite element simulation are slightly larger. This indicates that the finite element simulation is a reliable and safe method for settlement prediction.

In addition, the fact that the load settlement curves obtained from the static load test and the finite element simulation can be fitted also indicates that the finite element simulation of these four test piles is a valid simulation, which can provide more comprehensive information on the internal force and pile end deformation as a reference to verify the reliability of the method in this paper.

The settlement deformation in Z-direction obtained for each engineering test pile under the corresponding load is shown in Figure 14. The results show that the settlement of the soil near the pile perimeter is the largest, and a new compacted dense core area will be formed at the pile end, and a part of the soil will be settled below the compacted dense core area is relatively small. Combined with Figure 7, the soil settlement deformation trend near each pile end is consistent with that revealed by Janbu. Therefore, the ultimate pile end resistance calculation method referenced by the analytical equations proposed in this paper is appropriate.

Figure 15 shows the variation of axial force along the pile body at loading values of 1750 kN, 2100 kN, 2160 kN, and 2700 kN for test piles TS1, TS2, TS3, and TS4 extracted from the finite element model, respectively, and also shows the variation of axial force along the pile body at the vertical ultimate compressive load capacity for each test pile obtained by the calculation method in this paper. From a single test pile, the axial force of each part of the pile calculated by the method in this paper is generally larger compared with the results of finite element simulation, which is consistent with the actual situation, because the top load of the pile corresponding to the finite element simulation at this time does not reach the ultimate bearing capacity state that the pile can withstand. However, the trend of the axial force along the pile body is the same, and the axial force decreases gradually along the pile body. The reason is that the pile side frictional resistance of the shallow soil to the pile body is smaller, and a larger axial force is required to keep the pile body in a state of force equilibrium. The trend of the axial force along the pile body further illustrates that the vertical ultimate compressive load capacity calculation method proposed in this paper is a practical method in soft soil areas from the structural force characteristics.

6. Limitations and Future Works

The reliability of the analytical equations proposed in this paper for calculating the vertical ultimate compressive load capacity of monopiles in soft soil areas is verified from both numerical simulations and finite elements. The results show that the method in this paper is a simple and accurate method. This means that the method can be widely used for the prediction of ultimate bearing capacity of monopiles in soft soil areas, thus making it possible to reduce the number of static load tests, which can reduce certain costs for the project. However, the method also has some limitations.

(1) From the basic principle of the equation, the method can be extended to other types of soil areas. However, it is also necessary to consider whether the damage deformation characteristics of pile ends in other types of soil areas are similar to those in soft soil areas, and sufficient test data are needed to verify the reliability of the method

(2) In this paper, the ideal elastoplastic bifold model was chosen to describe the relationship between unit pile lateral friction resistance and pile-soil relative displacement, which is a basic and common model, but the model does not consider the softening effect between pile and soil. In future research, we can try to express the relationship between unit pile lateral frictional resistance and pile-soil relative displacement with a model that considers more influencing factors

Therefore, the new analytical equation proposed in this paper is used to calculate the vertical ultimate compressive bearing capacity of monopiles in soft soil areas with certain engineering value, but there is a need to do further research to make it produce more application value.

7. Conclusion

Based on all the research contents and results obtained in this study, the following conclusions can be drawn:

(1) Based on Randolph's study on the internal force of piles, a model for calculating the frictional resistance of pile segments in homogeneous soils considering the effect of self-gravity is proposed in this paper, and a method for calculating the internal force of piles in laminated soils is further derived. Combined with Janbu's research on ultimate end resistance, an analytical equation is proposed for calculating the vertical ultimate compressive bearing capacity of monopiles in soft soil areas. In order to verify the reliability of the method, static load tests and finite element simulations were carried out on four engineering test piles in the soft soil area of Suzhou, China

(2) The results show that the results of TS1, TS2, TS3, and TS4 for predicting the ultimate bearing capacity of monopiles in soft soil areas are in good agreement with the static load test results, and the error rate is only 1.57% if the results of the damaged test pile TS3 are taken to measure the deviation of the results. Finite element simulation was revealed from the two perspectives of pile end deformation characteristics and load transfer. the ultimate bearing capacity prediction method proposed in this paper based on Randolp's study of pile internal forces and Janbu's study of ultimate end resistance fits the actual situation and is an accurate and reliable method, which has important reference significance for other similar projects

Data Availability

The data used to support the findings of this study are available from the corresponding author upon request.

Conflicts of Interest

The authors declare that they have no conflicts of interest.

Acknowledgments

This study was supported by the Ministry of Industry and Information Technology of the People's Republic of China IoT Integrated Innovation and Convergence Application Project Fund (Grant Nos. 2018470) and Key R&D Projects in Shaanxi Province (No. 2020SF-373).

References

[1] Y. He, H. Hazarika, N. Yasufuku, J. Teng, Z. Jiang, and Z. Han, "Estimation of lateral force acting on piles to stabilize landslides," *Natural Hazards*, vol. 79, no. 3, pp. 1981–2003, 2015.

[2] F. Liang, H. Zhang, and M. Huang, "Extreme scour effects on the buckling of bridge piles considering the stress history of soft clay," *Natural Hazards*, vol. 77, no. 2, pp. 1143–1159, 2015.

[3] J. Krishnan and S. Shukla, "Shake table testing of liquefaction mitigation efficiency on pile foundations in sand stabilised with colloidal silica," *Natural Hazards*, vol. 111, no. 3, pp. 2317–2341, 2022.

[4] Z. Liu, Z. Yan, X. Wang, J. Li, and Z. Qiu, "Effect of the inclined pile-soil arch in a soil landslide reinforced with anti-sliding piles," *Natural Hazards*, vol. 106, no. 3, pp. 2227–2249, 2021.

[5] E. Conte, L. Pugliese, A. Troncone, and M. Vena, "A simple approach for evaluating the bearing capacity of piles subjected to inclined loads," *International Journal of Geomechanics*, vol. 21, no. 11, p. 04021224, 2021.

[6] L. Liu, H. Ma, X. Yang, Q. R. He, and S. Yuan, "A calculation method of bearing capacity of single squeezed branch pile based on load transfer method," *Advances in Materials Science and Engineering*, vol. 2022, Article ID 9597047, 9 pages, 2022.

[7] J. Guo, G. Dai, and Y. Wang, "Method for calculating vertical compression bearing capacity of the static drill rooted nodular pile," *Applied Sciences*, vol. 12, no. 10, p. 5101, 2022.

[8] S. Pu, Z. Zhu, and W. Song, "A method for calculating the ultimate bearing capacity of uplift piles in combined soil and rock mass," *European Journal of Environmental and Civil Engineering*, vol. 26, no. 6, pp. 2158–2183, 2022.

[9] E. Momeni, R. Nazir, D. J. Armaghani, and H. Maizir, "Prediction of pile bearing capacity using a hybrid genetic algorithm-based ANN," *Measurement*, vol. 57, pp. 122–131, 2014.

[10] R. Mohanty, S. Suman, and S. K. Das, "Prediction of vertical pile capacity of driven pile in cohesionless soil using artificial intelligence techniques," *International Journal of Geotechnical Engineering*, vol. 12, no. 2, pp. 209–216, 2018.

[11] W. Chen, P. Sarir, X. N. Bui, H. Nguyen, M. M. Tahir, and D. Jahed Armaghani, "Neuro-genetic, neuro-imperialism and genetic programing models in predicting ultimate bearing capacity of pile," *Engineering with Computers*, vol. 36, no. 3, pp. 1101–1115, 2020.

[12] Z. Luo, M. Hasanipanah, H. Bakhshandeh Amnieh, K. Brindhadevi, and M. M. Tahir, "GA-SVR: a novel hybrid data-driven model to simulate vertical load capacity of driven piles," *Engineering with Computers*, vol. 37, no. 2, pp. 823–831, 2021.

[13] H. Harandizadeh, M. M. Toufigh, and V. Toufigh, "Application of improved ANFIS approaches to estimate bearing capacity of piles," *Soft Computing*, vol. 23, no. 19, pp. 9537–9549, 2019.

[14] H. Harandizadeh, D. Jahed Armaghani, and M. Khari, "A new development of ANFIS–GMDH optimized by PSO to predict pile bearing capacity based on experimental datasets," *Engineering with Computers*, vol. 37, no. 1, pp. 685–700, 2021.

[15] S. Xiao, "A simplified approach for stability analysis of slopes reinforced with one row of embedded stabilizing piles," *Bulletin of Engineering Geology and the Environment*, vol. 76, no. 4, pp. 1371–1382, 2017.

[16] Z. Li, Z. Zhu, L. Liu, and L. Sun, "Distributions of earth pressure and soil resistance on full buried single-row anti-sliding piles in loess slopes in northern Shaanxi based on in-situ model testing," *Bulletin of Engineering Geology and the Environment*, vol. 81, no. 3, pp. 1–19, 2022.

[17] C. Wang, F. Liang, and X. Yu, "Experimental and numerical investigations on the performance of sacrificial piles in reducing local scour around pile groups," *Natural Hazards*, vol. 85, no. 3, pp. 1417–1435, 2017.

[18] G. Q. Kong, Q. Yang, H. L. Liu, and R. Y. Liang, "Numerical study of a new belled wedge pile type under different loading modes," *European Journal of Environmental and Civil Engineering*, vol. 17, no. sup1, pp. s65–s82, 2013.

[19] Z. H. Elsherbiny and M. H. El Naggar, "Axial compressive capacity of helical piles from field tests and numerical study," *Canadian Geotechnical Journal*, vol. 50, no. 12, pp. 1191–1203, 2013.

[20] R. Saggu and T. Chakraborty, "Cyclic thermo-mechanical analysis of energy piles in sand," *Geotechnical and Geological Engineering*, vol. 33, no. 2, pp. 321–342, 2015.

[21] M. J. Nowkandeh and A. J. Choobbasti, "Numerical study of single helical piles and helical pile groups under compressive loading in cohesive and cohesionless soils," *Bulletin of Engineering Geology and the Environment*, vol. 80, no. 5, pp. 4001–4023, 2021.

[22] X. Li, Y. Wang, Y. Hu, C. Zhou, and H. Zhang, "Numerical investigation on stratum and surface deformation in underground phosphorite mining under different mining methods," *Earth Science*, vol. 10, 2022.

[23] S. Xiong, C. Li, W. Yao, S. Yan, G. Wang, and Y. Zhang, "Physical model tests and numerical modeling of stabilizing mechanism of portal double-row piles in landslides with interbedded weak and hard bedrock," *Bulletin of Engineering Geology and the Environment*, vol. 81, no. 3, pp. 1–18, 2022.

[24] J. Dong, F. Chen, M. Zhou, and X. Zhou, "Numerical analysis of the boundary effect in model tests for single pile under lateral load," *Bulletin of Engineering Geology and the Environment*, vol. 77, no. 3, pp. 1057–1068, 2018.

[25] C. Wang, H. Wang, W. Qin, and H. Tian, "Experimental and numerical studies on the behavior and retaining mechanism of anchored stabilizing piles in landslides," *Bulletin of Engineering Geology and the Environment*, vol. 80, no. 10, pp. 7507–7524, 2021.

[26] M. Budhu, *Foundations and earth retaining structures*, John Wiley & Sons Incorporated, 2008.

[27] D. A. Brown, J. P. Turner, R. J. Castelli, and P. B. Americas, *Drilled shafts: construction procedures and LRFD design methods (no. FHWA-NHI-10-016)*, Federal Highway Administration, United States, 2010.

[28] A. Mishra, V. A. Sawant, and V. B. Deshmukh, "Prediction of pile capacity of socketed piles using different approaches," *Geotechnical and Geological Engineering*, vol. 37, no. 6, pp. 5219–5230, 2019.

[29] E. E. De Beer, "Proefondervindelijke bijdrage tot de studie van het gransdragvermogen van zand onder funderingen op staal," *Bepaling von der vormfactor sb, Annales des Travaux Publics de Belgique*, vol. 68, no. 6, pp. 481–506, 1967.

[30] F. K. Chin, "Estimation of the ultimate load of pile not carried to failure," in *Proceedings of the 2nd southeast Asian conference on soil engineering*, pp. 81–90, Singapore, 1970.

[31] L. Decourt, "Behavior of foundations under working load conditions," in *Proceedings of the 11th pan American conference on soil mechanics and Geotechnical engineering*, pp. 453–488, Foz Dulguassu, Brazil, 1999.

[32] H. Alielahi and M. Adampira, "Comparison between empirical and experimental ultimate bearing capacity of bored piles—a case study," *Arabian Journal of Geosciences*, vol. 9, no. 1, pp. 1–16, 2016.

[33] American Petroleum Institute (API), "Recommended practice for planning, designing, and constructing fixed offshore platforms-working stress design: upstream segment," in *API Recommended Practice 2A-WSD (RP 2A-WSD): Errata and Supplement 1, December 2002*, American Petroleum Institute, 2000.

[34] AASHTO, *Standard Specifications for Highway Bridges (2002) 17th Edition, HB-17*, American Association of State Highway and Transportation Officials, Washington, DC, 2002.

[35] M. Y. Abu-Farsakh and H. H. Titi, "Assessment of direct cone penetration test methods for predicting the ultimate capacity of friction driven piles," *Journal of Geotechnical and Geoenvironmental Engineering*, vol. 130, no. 9, pp. 935–944, 2004.

[36] J. R. Omer, R. Delpak, and R. B. Robinson, "A new computer program for pile capacity prediction using CPT data," *Geotechnical & Geological Engineering*, vol. 24, no. 2, pp. 399–426, 2006.

[37] F. S. Niazi and P. W. Mayne, "Cone penetration test based direct methods for evaluating static axial capacity of single piles," *Geotechnical and Geological Engineering*, vol. 31, no. 4, pp. 979–1009, 2013.

[38] A. M. A. Fateh, A. Eslami, and A. Fahimifar, "Direct CPT and CPTu methods for determining bearing capacity of helical piles," *Marine Georesources & Geotechnology*, vol. 35, no. 2, pp. 193–207, 2017.

[39] M. F. Randolph, "Design methods for pile groups and piled rafts," in *International conference on soil mechanics and foundation engineering*, vol. 5, pp. 61–82, New Delhi, 1994.

[40] N. Janbu, "Static bearing capacity of friction piles," in *Sechste Europaeische Konferenz Fuer Bodenmechanik Und Grundbau*, vol. 1, pp. 479–488, 1976.

[41] J. Yang, L. G. Tham, P. K. K. Lee, S. T. Chan, and F. Yu, "Behaviour of jacked and driven piles in sandy soil," *Géotechnique*, vol. 56, no. 4, pp. 245–259, 2006.

[42] F. H. Kulhawy, "Limiting tip and side resistance: fact or fallacy?," in *Analysis and design of pile foundations*, pp. 80–98, ASCE, 1984.

[43] Q. Q. Zhang, S. C. Li, F. Y. Liang, M. Yang, and Q. Zhang, "Simplified method for settlement prediction of single pile and pile group using a hyperbolic model," *International Journal of Civil Engineering*, vol. 12, no. 2, pp. 146–159, 2014.

[44] X. Liu and H. Zhu, "Experiment on interaction between typical soils in Shanghai and concrete," *Journal-Tongji University*, vol. 32, no. 5, pp. 601–606, 2004.

[45] M. W. O'Neill and R. D. Raines, "Load transfer for pipe piles in highly pressured dense sand," *Journal of Geotechnical Engineering*, vol. 117, no. 8, pp. 1208–1226, 1991.

[46] R. Jardine, F. Chow, R. Overy, and J. Standing, *ICP Design Methods for Driven Piles in Sands and Clays*, Thomas Telford, London, 2005.

[47] J. Cho, J. H. Lee, S. Jeong, and J. Lee, "The settlement behavior of piled raft in clay soils," *Ocean Engineering*, vol. 53, pp. 153–163, 2012.

[48] Q. Zhang, S. Liu, S. Zhang, J. Zhang, and K. Wang, "Simplified non-linear approaches for response of a single pile and pile groups considering progressive deformation of pile-soil system," *Soils and Foundations*, vol. 56, no. 3, pp. 473–484, 2016.

[49] F. Chen, T. Xu, G. Zhu et al., *Technical Code for Testing of Building Foundation Piles*, China Construction Industry Press, Beijing, China, 2014.